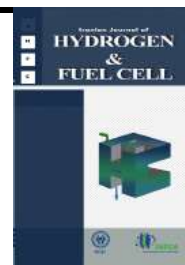


Iranian Journal of Hydrogen & Fuel Cell

IJHFC

Journal homepage://ijhfc.irost.ir



An experimental investigation on simultaneous effects of oxygen ratio and flow-rate in SOFCs performance fueled by a mixture of methane and oxygen

M. Farnak¹, J. A. Esfahani^{1,*}, S. Bozorgmehri²

¹Mech. Eng. Dept., Faculty of Eng., Ferdowsi University of Mashhad, Iran

²Renewable Energy Department, Niroo Research Institute (NRI), Tehran, Iran

Article Information

Article History:

Received:

05 May 2019

Received in revised form:

29 June 2019

Accepted:

10 July 2019

Keywords

Solid Oxide Fuel Cells (SOFCs)
Catalytic Partial Oxidation (CPOX)
Methane
Direct reforming
Reynolds number

Abstract

Catalytic partial oxidation (CPOX) has recently received particular attention because it is one of the most attractive technologies for the production of syngas and hydrogen in small to medium scales. Current study subjected to partial oxidation reforming which have simultaneously studied the effect of the fuel composition and flow rates of methane-oxygen mixed gas on the SOFCs performances. In this regard, the Reynolds number at the fuel channel inlet represents the mixture of methane and air mass flow rate. Moreover, the amount of oxygen ratio indicates the fuel composition. The results showed that the peak of power density (PPD) strongly depends upon both the Reynolds number at the fuel channel inlet and oxygen ratio. However, with the changes in Reynolds number or oxygen ratio, the oscillating behavior of PPD was observed. A dimensionless parameter can be introduced to take into account simultaneously the effect of oxygen ratio and Reynolds number of fuel on the PPD value. Considering the risk of carbon deposition as a constraint for selecting of oxygen ratio, the highest PPD corresponds to the methane/oxygen flow rates of 100/20 ccm for the applied methane/oxygen flow rates. The electrochemical experimental testing showed a stable performance of the SOFC in this condition and confirmed its durability after 120 hours testing. .

1. Introduction

A fuel cell is an electrochemical cell that converts the chemical energy from fuel into electricity through

an electrochemical reaction of hydrogen fuel with oxygen or another oxidizing agent. The conventional process of generating electricity from fuels involves several energy conversion steps:

*Corresponding Author's Fax: +985138806055

E-mail address: abolfazl@um.ac.ir

doi: 10.22104/ijhfc.2019.3591.1189

1. Conversion of the chemical energy of the fuels to thermal energy to boil water and generate steam,
2. Conversion of the thermal energy into mechanical energy by a turbine, and
3. Use the mechanical energy to run a generator that generates electricity.

However, a fuel cell circumvents all of these processes and generates electricity in a single step without involving moving parts. Additionally, electrochemical power generation has many advantages over fossil fuel combustion, including higher efficiency, zero/low pollution, limited equipment maintenance, and modularity [1].

Fuel cells are primarily classified by the kind of electrolyte they employ; hence, solid oxide fuel cells (SOFCs) are characterized by the use of a solid material as the electrolyte, i.e., Yttrium stabilized zirconia or YSZ. SOFCs have attracted a great deal of attention in the last few decades, mainly for their high energy conversion efficiency, limited emission levels, modularity, fuel flexibility, and low noise [2-4]. Conventional SOFCs employ a nickel-based anode (Ni-YSZ anodes) because of their various advantages. Unfortunately, carbon deposition occurs on nickel-based anodes when they are exposed to pure methane. This issue causes rapid degradation of the fuel cells. Reforming, a reaction of the hydrocarbon with oxygen-containing gases to produce a hydrogen/carbon monoxide mixture, of the actual cell fuel is standard practice to avoid the growth of carbon on nickel cermet anodes exposed to hydrocarbons. Moreover, the SOFC's high working temperatures provide additional positive features, such as the ability to internally reform different fuels (e.g. natural gas, propane, methanol, gasoline, diesel, etc.), to produce hydrogen for the electrical reaction [5-8]. In other words, internal reforming is an attractive option offering significant cost reduction, higher efficiencies, and faster load response with respect to traditional external reforming.

Three of the most economical ways to produce hydrogen from fossil fuels are steam-methane reforming (SMR), partial oxidation (POx), and autothermal reforming (ATR) [9-12]. Applying

conventional internal steam-reforming to Solid oxide fuel cells (SOFC) systems is not an appropriate method for decentralized synthesis gas production because steam reformers are large expensive plants that are difficult to scale down for small-scale operations in remote areas.

As an alternative to steam reforming, methane and other hydrocarbons may be converted to hydrogen via partial oxidation. Catalytic partial oxidation has recently received particular attention because it is one of the most attractive technologies for the production of syngas and hydrogen on a small to medium scale [13, 14]. Most of the literature in this field focuses on the effect of fuel composition on fuel cell performance, there are a limited number of works studying partial oxidation reforming and only a few of these have reviewed the effect of the flow rate of methane-oxygen mixed gases on the performance of SOFCs Lakshmi et al. [15] obtained the steady state characteristics of a fuel cell at different fuel flow rates ranging from 31 mL/s to 51 mL/s at two different operating temperatures 800 °C and 850 °C. It was observed that the limiting current density of fuel cell increases with the increase in fuel flow rate.

Lee et al. [16] demonstrated robust CPOX-based SOFCs fueled by CH₄, circumventing carbon coking and Ni oxidation. They showed that operation in a CH₄/O₂/N₂ fuel stream (CH₄:O₂:N₂ = 2:1:4, v/v) results in a maximum power density of 0.91 Wcm⁻² at 800 °C, while using H₂ and CH₄ gases led to values of 1.06 and 0.78 Wcm⁻², respectively. Buegler et al. [17] plotted the thermodynamic equilibrium gas mixture of a CH₄-air mixture for various CH₄/O₂ ratios as a function of temperature. They also calculated OCV for single-chamber SOFCs operating on CH₄-air mixtures with different CH₄/O₂ ratio, assuming perfect electrodes and purely ionic conducting electrolyte. Baldinelli et al. [18] investigated three levels of air-diluted natural gas, corresponding to an O/C equal to 1.2, 0.8 and 0.4. They reported voltage measurements for all the cells exposed to air-diluted natural gas mixtures. Their results showed that an O/C = 0.8 is the best dilution, from both a performances and material degradation

avoidance point of view. In the case of higher air-dilution ($O/C = 1.2$), nickel coarsening had already occurred after 100 h; but in the case of a lower dilution ($O/C = 0.4$), a constant-rate performance decay occurred. A consistent change in the zirconia lattice (tetragonal-to-monoclinic phase transition) which caused a loss in the ionic conductivity of the material was observed.

The dimensionless Reynolds number can play an important role in predicting and optimizing the performance of a fuel cell. Actually, the Reynolds number (Re) allows engineers to perform experiments using reduced scale models and then correlate the data to the actual flows thus saving on the cost of experimentation and lab time.

A conventional reactor based on steady-state flow and heterogeneous reactions catalyzed by solids is assumed for indirect internal reforming SOFCs (IIR-SOFC) fueled by natural gas [19]. As the flow condition affects the mass transfer and chemical reaction rate, the effect of the input fuel flow Reynolds number on the solid oxide fuel cell performance is important. Basically, the Re is dimensionless and describes the ratio of inertial to viscous forces for fluid flow and is calculated as follows:

$$Re = \frac{\rho V x}{\mu} \quad (1)$$

Where x , ρ , V , and μ are the spherical equivalent particle diameter, the density, the superficial velocity, and the viscosity of the methane and air mixture, respectively. The superficial velocity is the volumetric flow rate of the fluid divided by the cross sectional area of the reactor. The density of the mixture is calculated from the following equation in which y_1 and y_2 are the mole fraction of methane and air:

$$\rho_{mix} = y_1 \rho_1 + y_2 \rho_2 \quad (2)$$

Likewise, the model proposed by Wilke is used to calculate methane and air mixture viscosity [20]:

$$\mu_{mix} = \sum_{i=1}^n \frac{y_i \mu_i}{\sum_{j=1}^n y_j \phi_{ij}} \quad (3)$$

Where:

$$\phi_{ij} = \frac{\left[1 + \left(\frac{\mu_i}{\mu_j} \right)^2 \left(\frac{M_j}{M_i} \right)^{1/4} \right]^2}{\left[8 \left(1 + \left(\frac{M_i}{M_j} \right) \right) \right]^{1/2}} \quad \text{and} \quad \phi_{ji} = \frac{\mu_j M_i}{\mu_i M_j} \phi_{ij} \quad (4)$$

Where:

μ_{mix} = viscosity of the mixture

μ_i, μ_j = pure component viscosities

y_i, y_j = pure component mole fractions

M_i, M_j = pure component molecular weights

Laminar flow in a conventional packed-bed reactor occurs when the Reynolds number is below a critical value of approximately 10, though the transition range is typically between 10 and 2000. For such systems, fully turbulent flow exists at Reynolds numbers greater than around 2000 [21].

Moreover, the O_2/CH_4 ratio or oxygen ratio is the key parameter in the partial oxidation process. An oxygen ratio less than 0.2 maximizes the yield in hydrogen. However, fuel cell failure is expected because of the high risk of carbon deposition in this ratio. The risk of carbon deposition is reduced by selecting an oxygen ratio in the range of 0.2-0.3, which allows both the equilibrium temperature and desired hydrogen conversion to be obtained even with low pre-heating of the inlet reactant mixture [1]. However, the smaller yield in hydrogen, with respect to the theoretical condition, could be a disadvantage of this ratio. An oxygen ratio greater than 0.3 is used in the startup phases to stabilize the reactor temperature. Although this leads to higher methane conversion, the hydrogen yield is lower than in other conditions.

If the carbon deposition issue is ignored (which is clearly impossible), the behavior of the cell is similar to that of the hydrogen-fueled SOFC for a low amount of oxygen added to methane during CPOX. A high CH_4/O_2 ratio can theoretically guarantee the highest hydrogen conversion, but the risk of undergoing carbon deposition over the catalyst bed (and also the anode cell) is high. This implies there is a risk that the methane does not react with

the air to yield hydrogen and carbon monoxide by the reforming reaction. Instead, it tends to pyrolysis forming coke and facilitating the carbon deposition. In other words, the proper selection of oxygen ratio plays an important role in SOFC performance.

In addition, the oxygen ratio affects the OCV value according to the Nernst equation. Nernst law states the maximum possible OCV depends on the difference between the anode and cathode oxygen concentration. It can be calculated from the partial pressure of the oxygen at the cathode $P_C(O_2)$ and at the anode $P_A(O_2)$ [22].

$$OCV = \frac{-\Delta G}{nF} = \frac{RT}{nF} \ln \left(\frac{P_C(O_2)}{P_A(O_2)} \right) \quad (5)$$

In this equation, R is the gas constant (J/mol.K), T is the absolute temperature (K), F is the Faraday constant (A.s/mol), and n is the electron equivalent of oxygen. The partial pressure of the oxygen is 0.21 atm at the cathode, and the partial pressure of the oxygen is dependent on temperature and fuel composition at the anode [17].

Only a limited number of works investigate the effect of the Reynolds number of fuel flow on SOFCs performance. Ozgur Colpan et al. [23] present the development of a new transient heat transfer model of a planar solid oxide fuel cell (SOFC) operating with humidified hydrogen. They showed that a low Reynolds number gets better electrical efficiencies. Iora et al. [24] compares two dynamic one-dimensional models of a planar anode-supported intermediate temperature (IT) direct internal reforming (DIR) solid oxide fuel cell (SOFC). They showed that the Reynolds number in the air channel is one order of magnitude larger than in the fuel channel, due to an order-of-magnitude difference in velocities.

In the present study, oxygen was added into the fuel for the internal catalytic partial oxidation reforming of methane over the Ni-YSZ cermet anode of solid oxide fuel cells (SOFCs) to study the advantages of partial oxidation. For the first time, both the effect of fuel composition and fuel flow rate on the SOFC power density was simultaneously considered experimentally. In this regard, the Reynolds number

at the fuel channel inlet represents the mixture of methane and air mass flow rate and the amount of the oxygen ratio indicates the fuel composition.

2. Materials and methods

The anode-supported button cells composed of NiO/YSZ anodes, YSZ membranes, LSM cathodes and a diffusion barrier layer with diameter of 2.5 cm were purchased from SOFC MAN, China. The anode substrate was a layer made of dense nickel oxide and porous nickel-YSZ cermet with a thickness of approximately 400 μm . The electrolyte and cathode were, in order, a dense YSZ layer with a thickness of 10-15 μm and a Strontium-doped Lanthanum Manganite (LSM) layer with a thickness of 20-25 μm . Also, the diffusion barrier substrate was a layer fabricated of Gadolinium-doped ceria (GDC) with a 2-3 μm thickness. It is worth noting that combining GDC with the Ni anode prevents the oxidation of Ni due to the oxygen exchange ability of GDC. SOFC tests were carried out in a single cell test setup similar to that used by many groups [25]. The reactor cell was arranged onto an apparatus which involves cylinders with all the necessary gases, i.e., O_2 , CH_4 , He, H_2 and Ar. The cathode was fed with air and the anode was operated with a methane/oxygen mixture for the internal reforming. The purity of the applied Oxygen was 99.95%. Furthermore, the gas grade purity specifications (Methane, Research Purity 99.999%) are as shown in Table 1.

Table 1. The gas grade purity specifications.

Chemical Parameter	Purity Specification	Unit
Methane	99.999	%
Ethane	2	ppm
Propane	0.5	ppm
Nitrogen	3	ppm
Oxygen	0.5	ppm
Other Hydrocarbons	0.5	ppm
Carbon Dioxide	0.5	ppm
Moisture	0.5	ppm

The silver paste was applied on both sides of the cell

with an extended silver mesh (current collector) with an active area of 1 cm^2 . Silver mesh and silver paste served as the output terminals and current collectors of the electrodes, respectively. Cement seal was used to seal the cell in contact with the alumina tube. A quartz tube was also used for delivering the gas to

the cell. A schematic view of the experimental setup and gas fuel mixture handling for a single cell test setup is displayed in Figs. 1 (a, b). The oxygen flow was regulated by a gas mass flow controller and was injected directly into the hot fuel. The gas flows were adjusted by means of mass flow controllers.

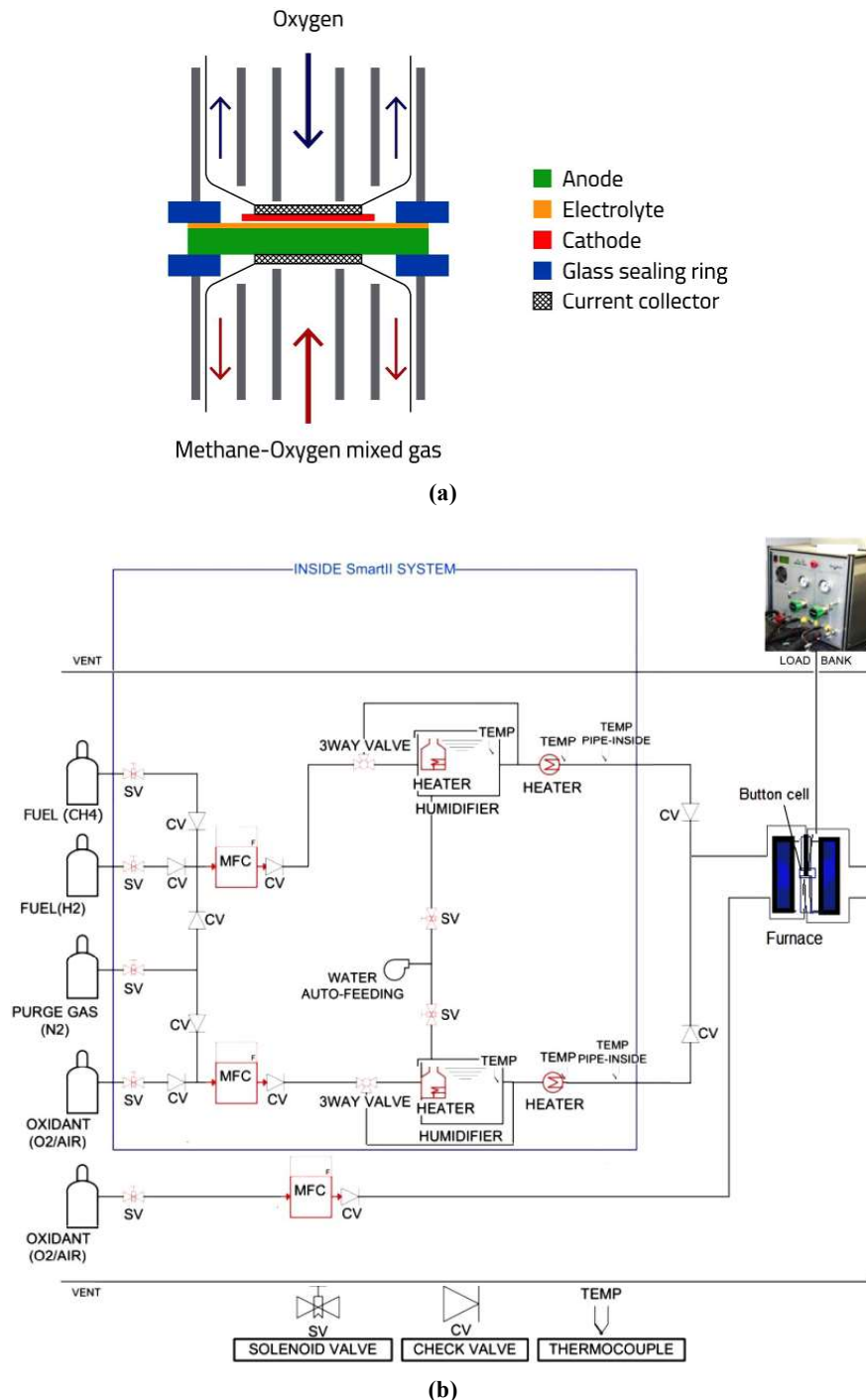


Fig. 1 Schematic view of experimental setup (a) and gas fuel mixture handling unit (b).

After reaching a temperature of 800°C, nitrogen was purged into the test rig for about 5 min in order to remove any impurities and air in the test setup. For reducing and activating the NiO in the anode, a N₂-5% H₂ gas mixture was applied for about two hours to reach to the steady potential of the cell. Then, pure hydrogen was purged to the cells in order to complete the anode activating procedure. Finally, oxygen mixed with methane was utilized for the cell performance experiment. The applied flow rates for the partial oxidation reforming process were methane/oxygen flow rates of 150/10, 100/20, 150/30, 200/40, 300/60, 400/40, 200/80 and 50/30 ccm. WonATech SMARTII was used for gas handling and electrochemical evaluation. Linear sweep voltammetry (LSV) at a scan rate of 10 mV/S and chronopotentiometry were employed to investigate the electrochemical performance of the cells. The flow rate of the oxygen at the cathodic side was adjusted to equal the flow rate of the fuel purged into the anodic side of the SOFCs. The durability of the button cell was subsequently tested for 120 hours at a current density of 0.2 A/cm².

3. Results and discussion

First, the nickel oxide was reduced to metal under hydrogen in order to provide a percolation path for electrons through the anode. After the reduction process, the OCV reached 1.12 V at a flow rate of 150 ccm of pure hydrogen and then did not change any further with the flow rate. At this point, the electrochemical analyses were done at 800°C.

Fig. 2 compares the I-V plot of SOFC operated under a flow rate of 150 ccm pure methane and pure hydrogen fuels. According to this figure, the methane and hydrogen electrochemical characterization are quite similar. The maximum power densities are 0.55 and 0.53 at a current density of 1 A/cm² for pure hydrogen and pure methane, respectively.

Furthermore, their OCV values are very close together. However, it has been proven that carbon deposition leads to fast degradation of the cell under

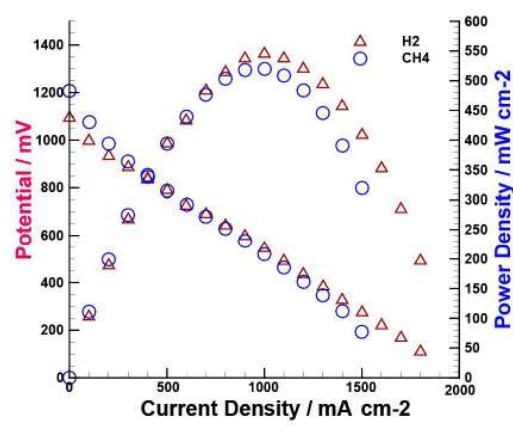


Fig. 2. I-V plot of SOFC button cell operated under a flow rate of 150 ccm pure methane and pure hydrogen fuels

pure methane feeding conditions over long periods of time [26].

Fig. 3 shows the I-V plot for applied methane/oxygen flow rates. The calculated Re number of fuel flow for the methane/oxygen flow rate ratio of 150/10, 100/20, 400/40, 150/30, 200/40, 300/60, 50/30 and 200/80 are 10, 10.34, 29.83, 15.51, 20.68, 31.02, 10.93 and 32.21, respectively. The related parameters for the calculation of a typical Reynolds number are included in appendix A.

The applied flow rate values were selected in the range of Reynolds number =10-30 in which the transient flow are dominant.

As it can be seen in Fig. 3, the I-V variation shows linear behavior at moderate current densities (for current densities greater than 100 mA/cm²), which corresponds to ohmic loss by applying current at a high operating temperature of 800°C. The ohmic losses in internal electrochemical systems of SOFC are generally due to the material and fabrication specifications of the SOFCs, e.g., the thickness of cell components and the electrical conductivity of the materials. So, the cell performance should be independent of the flow rates. The same slopes of the I-V plots in the mid-region of the current densities confirmed this independency. Purging more than the optimum fuel flow rates is associated with increasing of activation polarization due to the higher required over potential for activating the electrochemical reactions.

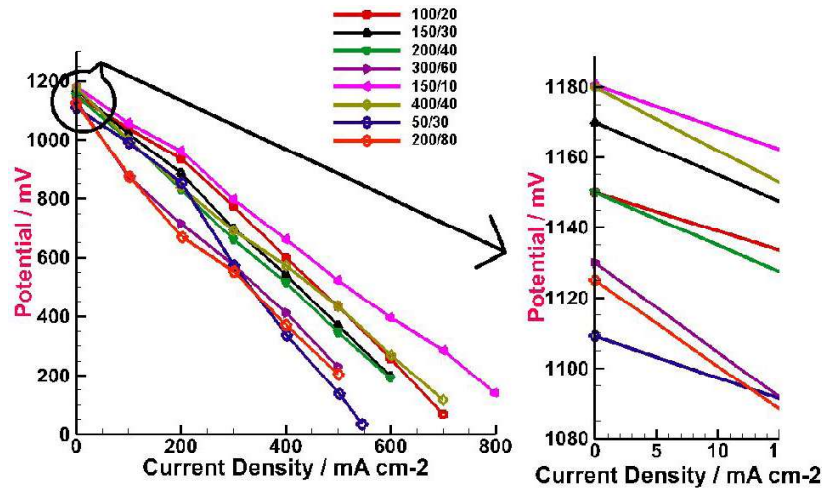


Fig 3. The I-V plots for SOFC during partial oxidation reforming with methane: oxygen flow rates of 150/10, 100/20, 400/40, 150/30, 200/40, 300/60, 50/30 and 200/80 ccm

Moreover, the OCV for the flow rates of 150/10, 400/40, 200/400 and 50/30 are 1.18, 1.17, 1.13 and 1.11, respectively [17]. Considering Nernst's equation (Eq. 5), the OCV values are expected to be the same for all the different flow rates of oxygen and methane with the same oxygen ratio. This fact is also confirmed clearly by the experimentally measured OCV shown in Fig. 3. Furthermore, Fig. 3 also shows that the experimentally measured OCV is 1.15 ± 0.02 V for all of the different flow rates of oxygen and methane with an oxygen ratio of 1:5. In fact, the observed difference (~ 0.02 V) for the OCV measurements can be due to random error. Random error incorporates all other sources of variability in the experiment including measurement, variability arising from uncontrolled factors, etc. Considering the most and least oxygen concentration difference between anode and cathode, the most and least OCV are obtained in the methane/oxygen flow rates of 150/10 and 50/30, respectively.

Fig. 4 shows the I-P plots for methane/oxygen flow rates of 50/10, 100/20, 150/30, 200/40, 300/60 and 400/80 sccm, the maximum points were selected as PPDs. Then, the obtained PPDs vs Reynolds number of fuel flow are plotted in Fig. 5. According to this figure, increasing the Re number of fuel flow causes the PPD values to fluctuate severely. Hence, increasing the fuel supply does not necessarily increase the performance of SOFCs. During

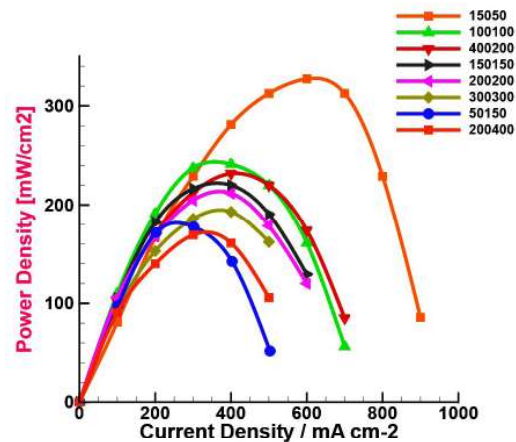


Fig. 4. The power density plots for SOFC during partial oxidation reforming with methane: oxygen flow rates of 150/10, 100/20, 400/40, 150/30, 200/40, 300/60, 50/30 and 200/80 ccm

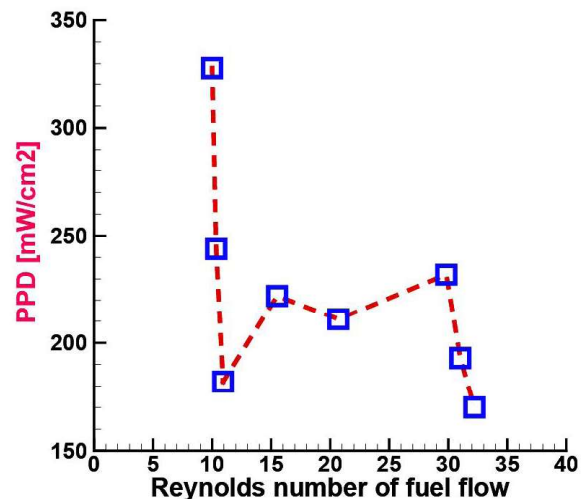


Fig. 5. The obtained PPD vs Reynolds number of fuel flow

operation of a SOFC, two effects intervene to reduce the electrical power available from an ideal cell; the first is ohmic resistance which generates heat and the second is the irreversible mixing of gases which causes the voltage to fall as progressively more fuel is used in the reaction. Essentially, this means that a SOFC cannot realistically use all of the fuel (fuel utilization). In fact, increasing the Reynolds number can increase the mass transfer, total reaction rate, and subsequently the PPD [21]. However, in addition to a decrease in mean residence time for SOFC fluid in the transitional region with $10 < Re < 2000$, the reaction products are hardly desorbed from the surface which causes a PPD reduction. However, the concentration of species (i.e. the oxygen ratio) can be effective in (increasing, decreasing?) the severity of desorption from the catalytic surface. Therefore, the swinging changes of PPD values with increasing Re implies the dual effect of Reynolds number and oxygen ratio on PPD.

Moreover, the PPD changes with oxygen ratio are showed in Fig. 6. There are several quantities of PPD in various flow rates with the same oxygen ratio equal to 0.2. At oxygen ratio equal to 0.2, the PPD lowered from 0.244 to 0.193 W/cm² when increasing the Reynolds number of fuel flow. Therefore, by increasing Re at a constant oxygen ratio, the effect of slow desorption from the catalytic surface has been overcome by the fast reaction rate. In other words, the PPD is inversely proportional to the Re number of fuel flow. However, at a constant Reynolds number of fuel flow equal to 10, the PPD increased from 0.182 to 0.328 W/cm² due to a decrease in the oxygen ratio. Consequently, it can be concluded that the PPD is also inversely proportional to the oxygen ratio.

So, it is useful to define a dimensionless parameter such as Φ to simultaneously take into account the effect of the oxygen ratio and Reynolds number of fuel on the PPD value as follows;

$$\Phi = \frac{\beta}{Re} \quad \text{and} \quad \beta = \frac{1}{\text{air ratio}} \quad (6)$$

The PPD vs Φ is displayed in Fig. 7. According to this

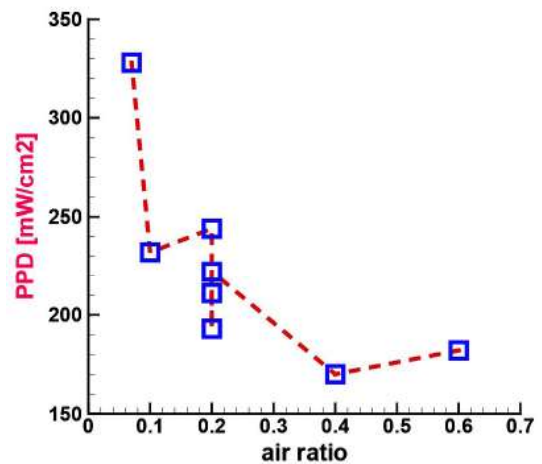


Fig. 6. The obtained PPD vs Reynolds number of fuel flow.

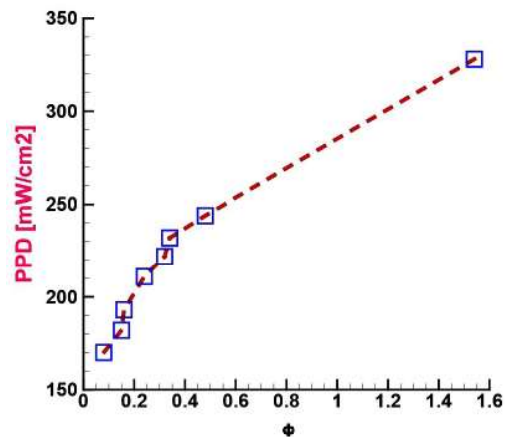


Fig. 7. The PPD vs Φ .

figure, the PPD increases continuously as Φ increases. On the other hand, a decrease in the Re number of fuel flow and oxygen ratio increases PPD. Therefore, SOFC performance prediction is possible due to the lack of fluctuation in Φ behavior. Nevertheless, the selection of the oxygen ratio is constrained in the range of 0.2-0.3 due to the risk of carbon deposition. The highest PPD value of 0.328 W/cm² is seen at the $\Phi = 1.54$ for a fuel flow rate of 150 ccm methane and 10 ccm oxygen. However, the oxygen ratio for this fuel condition (0.07) is not in the range of 0.2 to 0.3. Consequently, for the applied methane/oxygen flow rates, the highest Φ satisfying the oxygen ratio constraint is 0.48, which corresponds to the methane/oxygen flow rates of 100/20 ccm. However, if a long-term test was not carried out, the durability of the cell at this working condition is doubtful. As it is clearly

impossible to perform a long-term test for an infinite time, 120 h seems to be a reasonable time according to many articles.

Fig. 8 represents the V-t plot for SOFC in a mixture of methane and oxygen at a loading of 0.2 A/cm^2 for 120 hours. As can be seen in the figure, the voltage of the cell decreased to $0.53 \pm 0.02 \text{ V}$ during the first hour. In fact, after switching the fuel from pure hydrogen to the pre-defined flow mixtures of methane and oxygen, the cell performance naturally dropped. It is noted that the fastest reaction at the nickel anode is that of hydrogen. The other fuels can also react directly on the anode but have a higher overpotential than hydrogen. This drop in potential was also observed by Lin et al. [25]. They investigated the direct-methane operation of Ni-YSZ anode-supported SOFCs and reported that the V value at constant current density dropped by $\approx 20\%$ to a new steady state value after pure hydrogen was switched to methane. Furthermore, there are many other studies that reported the same range value for the operating voltage in SOFCs. Lin et al. [25] plotted cell voltage versus time at constant current density for SOFCs operating in humidified methane at various temperatures for about 300 min. Their cells voltage varied between 0.58 and 0.71 depending on the current density values. Additionally, Pillai et al. [27] displayed the voltage versus time for a SOFC operated at 800°C with a fuel mixture of 75% CH_4 and 25% air (30 ccm CH_4 and 10 ccm air). Their results showed variation of the cell voltage between 0.55 and 0.83 V. Fig. 8 also shows that a gradually increase occurred in the potential at $0.63 \pm 0.02 \text{ V}$ after about three hours. Following that the potential remains almost constant with very small oscillation amplitudes, which may indicate that intense Ni/NiO redox cycles did not take place on the Ni-anode.

4. Conclusion

The effect of the Reynolds number of the fuel flow and the oxygen ratio on the electrochemical performance of a solid oxide fuel cell was simultaneously

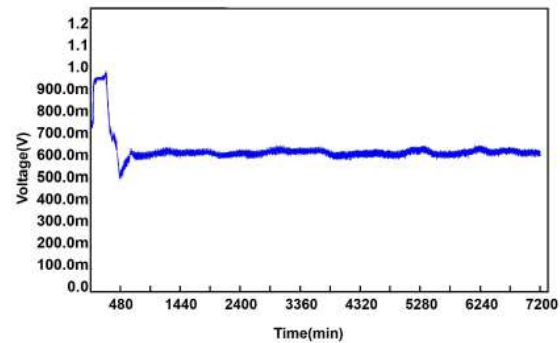


Fig. 8. The V-t plot for SOFC in a mixture of methane and oxygen at loading of 0.2 A/cm^2 for 120 hours

evaluated in catalytic partial oxidation conditions.

It was shown that there are insignificant measurements in OCV for different flow rates of methane/oxygen with a fix oxygen ratio at 800°C . However, the maximum and minimum OCV were obtained in the methane/oxygen flow rates of 150/10 and 50/30, respectively. Furthermore, it was observed that PPD values fluctuated severely when increasing the Re number of fuel flow. Moreover, there are several quantities for PPD in various flow rates with the same oxygen ratio. A dimensionless parameter such as Φ is introduced to simultaneously take into account the effect of oxygen ratio and Reynolds number of fuel on the PPD value. It was found that SOFC performance prediction is possible due to the lack of fluctuation in Φ behavior. For the applied methane/oxygen flow rates, the highest value of Φ which satisfies the range of oxygen ratio between 0.2 and 0.3 corresponds to the methane/oxygen flow rate of 100/20 ccm.

Durability testing of the cell in this condition showed good cell performance stability after 120 h.

Appendix A

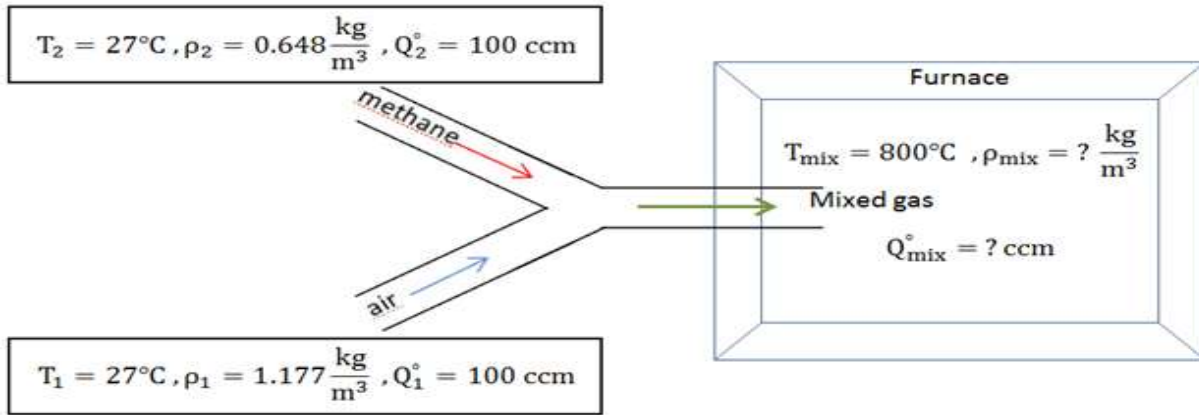
The calculations are presented here for methane/oxygen flow rate of 100/20 sccm (or methane/air flow rate of 100/100 sccm).

$$@T_{\text{mix}}=800^\circ\text{C}; \rho_{\text{air},T_{\text{mix}}}=0.3292 \text{ kg/m}^3$$

$$@T_{\text{mix}}=800^\circ\text{C}; \rho_{\text{methane},T_{\text{mix}}}=0.179761 \text{ kg/m}^3$$

$$y_1=\text{pure component mole fractions of air} = 0.5$$

$$y_2=\text{pure component mole fractions of methane} = 0.5$$



$$\rho_{\text{mix}} = y_1 \rho_{\text{air}, T_{\text{mix}}} + y_2 \rho_{\text{methane}, T_{\text{mix}}} = 0.5 \times 0.179761 + 0.5 \times 0.3292 = 0.2544805 \text{ kg/m}^3 \quad (1)$$

$$Q_{\text{mix}} = \frac{(\dot{n}_1 Q_1 + \dot{n}_2 Q_2)}{\dot{n}_{\text{mix}}} = \frac{1.177 \times 100 + 0.64838845 \times 100}{0.2544805} = 717.3 \text{ sccm} = 11.95 \times 10^{-6} \frac{\text{m}^3}{\text{s}}$$

The tube used for delivering the gas to the cell has a diameter of 1 centimeter;

$$A = 0.25 \pi (0.01)^2 = 0.79 \times 10^{-4} \text{ m}^2$$

$$v_{\text{mix}} = \frac{Q_{\text{mix}}}{A} = \left(\frac{11.95 \times 10^{-6}}{0.79 \times 10^{-4}} \right) = 0.1522 \frac{\text{m}}{\text{s}} \quad (2)$$

$$@T_{\text{mix}} = 800^\circ\text{C}; \mu_{\text{air}, T_{\text{mix}}} = 4.331 \times 10^{-5} \text{ Pa.s}$$

$$@T_{\text{mix}} = 800^\circ\text{C}; \mu_{\text{methane}, T_{\text{mix}}} = 3.01 \times 10^{-5} \text{ Pa.s}$$

Molecular weight of methane = $M_{\text{methane}} = 16.043$ gr/mol

Molecular weight of air = $M_{\text{air}} = 28.965$ gr/mol

$$\begin{aligned} \phi_{12} &= \frac{\left[1 + \left(\frac{\mu_{\text{methane}}}{\mu_{\text{air}}} \right)^{1/2} \left(\frac{M_{\text{air}}}{M_{\text{methane}}} \right)^{1/4} \right]^2}{\left[8 \left(1 + \left(\frac{M_{\text{methane}}}{M_{\text{air}}} \right) \right) \right]^{1/2}} = \\ &= \frac{\left[1 + \left(\frac{3.01 \times 10^{-5}}{4.331 \times 10^{-5}} \right)^{1/2} \left(\frac{28.965}{16.043} \right)^{1/4} \right]^2}{\left[8 \left(1 + \left(\frac{16.043}{28.965} \right) \right) \right]^{1/2}} = 1.096 \end{aligned}$$

$$\phi_{21} = \frac{\mu_{\text{air}}}{\mu_{\text{methane}}} \frac{M_{\text{methane}}}{M_{\text{air}}} \phi_{12} = \frac{4.331 \times 10^{-5}}{3.01 \times 10^{-5}} \times \frac{16.043}{28.965} \times 1.096 = 0.8739$$

$$\mu_{\text{mix}} = \frac{\sum_{i=1}^n y_i \mu_i}{\sum_{j=1}^n y_j \phi_{ij}} = \frac{y_1 \mu_{\text{methane}}}{y_1 + y_2 \phi_{12}} + \frac{y_2 \mu_{\text{air}}}{y_2 + y_1 \phi_{21}} =$$

$$\frac{0.5 \times 3.01 \times 10^{-5}}{0.5 + 0.5 \times 1.096} + \frac{0.5 \times 4.331 \times 10^{-5}}{0.5 + 0.5 \times 0.8739} = 3.747 \times 10^{-5} \text{ Pa.s}$$

The following equation was applied for the calculation of equivalent particle diameter as bellow:

$$\varepsilon = \frac{\text{volume of voids}}{\text{total volume}}$$

Active area of cell = 1 cm^2

The anode thickness = $400 \mu\text{m}$

Total volume = $1 \times 400 = 400 \times 10^{-8} \text{ m}^3$

The mean void fraction of 0.4 was measured by Image-J analysis software.

$$(1 - \varepsilon)(\text{total volume}) = \frac{\pi d_{\text{eq}}^3}{6} \Rightarrow d_{\text{eq}} \cong 0.01 \text{ m} \quad (4)$$

From Eq. (1) to (4):

$$Re = \frac{\rho v d}{\mu} = \frac{0.25 \times 0.15 \times 0.01}{3.747 \times 10^{-5}} = 10$$

References

[1] A. Di Filippi, Development and experimental validation of CPOx reforming dynamic model for fault detection and isolation in SOFC systems, (2015).

- [2] M. Sorrentino, C. Pianese, Control oriented modeling of solid oxide fuel cell auxiliary power unit for transportation applications, *Journal of Fuel Cell Science and Technology*, 6 (2009) 041011.
- [3] D. Hickman, L.D. Schmidt, Steps in CH₄ oxidation on Pt and Rh surfaces: High-temperature reactor simulations, *AIChE Journal*, 39 (1993) 1164-1177.
- [4] S.C. Singhal, K. Kendall, High-temperature solid oxide fuel cells: fundamentals, design and applications, Elsevier, (2003) 1-20.
- [5] M. Sorrentino, Development of a hierarchical structure of models for simulation and control of planar solid oxide fuel cells, Department of Mechanical Engineering, University of Salerno, Italy, (2006).
- [6] H. Zhang, J. Chen, J. Zhang, Performance analysis and parametric study of a solid oxide fuel cell fueled by carbon monoxide, *International Journal of Hydrogen Energy*, 38 (2013) 16354-16364.
- [7] H. Xu, B. Chen, H. Zhang, W. Kong, B. Liang, M. Ni, The thermal effect in direct carbon solid oxide fuel cells, *Applied Thermal Engineering*, 118 (2017) 652-662.
- [8] S. Cordiner, M. Feola, V. Mulone, F. Romanelli, Analysis of a SOFC energy generation system fuelled with biomass reformat, *Applied Thermal Engineering*, 27 (2007) 738-747.
- [9] L. Fan, L. Van Biert, A.T. Thattai, A. Verkooijen, P. Aravind, Study of methane steam reforming kinetics in operating solid oxide fuel cells: influence of current density, *International Journal of Hydrogen Energy*, 40 (2015) 5150-5159.
- [10] Y. Wang, F. Yoshida, M. Kawase, T. Watanabe, Performance and effective kinetic models of methane steam reforming over Ni/YSZ anode of planar SOFC, *International Journal of Hydrogen Energy*, 34 (2009) 3885-3893.
- [11] V. Liso, G. Cinti, M.P. Nielsen, U. Desideri, Solid oxide fuel cell performance comparison fueled by methane, MeOH, EtOH and gasoline surrogate C₈H₁₈, *Applied Thermal Engineering*, 99 (2016) 1101-1109.
- [12] Y. Yang, X. Du, L. Yang, Y. Huang, H. Xian, Investigation of methane steam reforming in planar porous support of solid oxide fuel cell, *Applied Thermal Engineering*, 29 (2009) 1106-1113.
- [13] M. Martinelli, Application of the spatially resolved sampling technique to the analysis and optimal design of a CH₄-CPO reformer with honeycomb catalyst, University of POLITECNICO DI MILANO, Faculty of Engineering of Industrial Processes Department of Energy, Phd Thesis (2011), 5-121.
- [14] S. Sui, G. Xiu, 14-Fuels and fuel processing in SOFC applications, in: *High-temperature Solid Oxide Fuel Cells for the 21st Century*, Academic Press Boston, (2016) 461-495.
- [15] T. Lakshmi, P. Geethanjali, P.S. Krishna, Mathematical modelling of solid oxide fuel cell using Matlab/Simulink, in: *2013 Annual International Conference on Emerging Research Areas and 2013 International Conference on Microelectronics, Communications and Renewable Energy*, IEEE, (2013) 1-5.
- [16] D. Lee, J. Myung, J. Tan, S.-H. Hyun, J.T. Irvine, J. Kim, J. Moon, Direct methane solid oxide fuel cells based on catalytic partial oxidation enabling complete coking tolerance of Ni-based anodes, *Journal of Power Sources*, 345 (2017) 30-40.
- [17] B.E. Buegler, A.N. Grundy, L.J. Gauckler, Thermodynamic equilibrium of single-chamber SOFC relevant methane-air mixtures, *Journal of The Electrochemical Society*, 153 (2006) A1378-A1385.
- [18] A. Baldinelli, L. Barelli, G. Bidini, A. Di Michele, R. Vivani, SOFC direct fuelling with high-methane gases: Optimal strategies for fuel dilution and upgrade to avoid quick degradation, *Energy Conversion and Management*,

124 (2016) 492-503.

[19] F. Priyakorn, N. Laosiripojana, S. Assabumrungrat, Modeling of solid oxide fuel cell with internal reforming operation fueled by natural gas, *Journal of Sustainable Energy & Environment*, 2 (2011) 187-194.

[20] B.E. Poling, J.M. Prausnitz, J.P. O'Connell, *The properties of gases and liquids*, Mcgraw-hill New York, 2001.

[21] M.J. Rhodes, M. Rhodes, *Introduction to particle technology*, John Wiley & Sons, 2008.

[22] O. Yamamoto, Solid oxide fuel cells: fundamental aspects and prospects, *Electrochimica acta*, 45 (2000) 2423-2435.

[23] C.O. Colpan, F. Hamdullahpur, I. Dincer, Transient heat transfer modeling of a solid oxide fuel cell operating with humidified hydrogen, *International Journal of Hydrogen Energy*, 36 (2011) 11488-11499.

[24] P. Iora, P. Aguiar, C. Adjiman, N. Brandon, Comparison of two IT DIR-SOFC models: Impact of variable thermodynamic, physical, and flow properties. Steady-state and dynamic analysis, *Chemical Engineering Science*, 60 (2005) 2963-2975.

[25] Y. Lin, Z. Zhan, J. Liu, S.A. Barnett, Direct operation of solid oxide fuel cells with methane fuel, *Solid State Ionics*, 176 (2005) 1827-1835.

[26] H. Aslannejad, L. Barelli, A. Babaie, S. Bozorgmehri, Effect of air addition to methane on performance stability and coking over NiO-YSZ anodes of SOFC, *Applied Energy*, 177 (2016) 179-186.

[27] M. Pillai, Y. Lin, H. Zhu, R.J. Kee, S.A. Barnett, Stability and coking of direct-methane solid oxide fuel cells: Effect of CO₂ and air additions, *Journal of Power Sources*, 195 (2010) 271-279.